

# New Compatibilizer for Linear Low-Density Polyethylene (LLDPE)/Clay Nanocomposites

Dong-Woo Jin, Sung-Mok Seol, Gue-Hyun Kim

Division of Applied Bio Engineering, Dongseo University, Busan 617-716, South Korea

Received 30 November 2008; accepted 5 April 2009

DOI 10.1002/app.30544

Published online 27 May 2009 in Wiley InterScience (www.interscience.wiley.com).

**ABSTRACT:** Linear low-density polyethylene (LLDPE) is one of the most widely used polymers in many fields, but it is difficult to prepare LLDPE/clay nanocomposites because of the hydrophobic nature of LLDPE. In this study, the effectiveness of low molecular weight trimethoxysilyl-modified polybutadiene (Organosilane) as a compatibilizer for LLDPE/clay nanocomposites was studied using X-ray diffraction (XRD) and correlated with mechanical properties. Organosilane is known to react with dicumyl peroxide (DCP) to form free radicals, which react

with LLDPE increasing the polarity of the LLDPE. Based on XRD and mechanical tests, it was concluded that Organosilane is a good compatibilizer for LLDPE and clay. Also when Organosilane was used in preparing LLDPE/clay nanocomposite foams, most mechanical properties were improved. © 2009 Wiley Periodicals, Inc. *J Appl Polym Sci* 114: 25–31, 2009

**Key words:** nanocomposites; clay; mechanical properties; miscibility; polyolefins

## INTRODUCTION

Linear low-density polyethylene (LLDPE) is one of the most widely used polyolefins in many fields. However, its low-mechanical strength and low-thermal resistance sometimes limit some industrial applications. Thus, to improve the mechanical strength, fillers are mixed with LLDPE. In recent years, clay-based polymer nanocomposites have attracted considerable attention from the field of fundamental research and from the field of research on various applications, because of the remarkable capacity of clay to improve nanocomposite properties. Owing to the thickness of the nanometer dimension and the extremely high aspect ratio of the silicate layers, these nanocomposites exhibit dramatic improvements in mechanical, thermal, and barrier properties.<sup>1–12</sup>

However, it is very difficult for hydrophobic polymers such as LLDPE to intercalate into clay layers because LLDPE has no polar groups in the backbone of its chain. Therefore to improve the interaction between LLDPE and clay, maleic anhydride grafted LLDPE has been widely used as a compatibilizer in most studies, because it has good miscibility with LLDPE and contains polar functional groups that can interact with the polar clays.

In this study, the effectiveness of low molecular weight trimethoxysilyl-modified polybutadiene (Organosilane) as a compatibilizer was studied and correlated with mechanical properties. Organosilane is known to react with dicumyl peroxide (DCP) to form free radicals,<sup>13–19</sup> which react with LLDPE, increasing the polarity of the LLDPE.<sup>20,21</sup> Also, LLDPE/Organosilane/clay nanocomposite foams were prepared, and their mechanical properties were investigated.

## EXPERIMENTAL

### Materials and preparation of nanocomposite

Names and important characteristics of the materials used in this study are summarized in Table I. Unmodified montmorillonites and organically modified montmorillonites were purchased from Southern Clay Products (Austin, TX) under the trade name of Cloisite Na<sup>+</sup>, Cloisite 20A, and Cloisite 30B. Organic modifier of Cloisite 20A is dimethyl dihydrogenated tallow quaternary ammonium and organic modifier of Cloisite 30B is methyl tallow bis-2-hydroxyethyl quaternary ammonium. LLDPE, clay, Organosilane, zinc oxide (3 phr), and stearic acid (1 phr) were mixed in a Haake internal mixer at 165°C for 5 min and then DCP was added to the mixer. Total mixing time was 10 min. Obtained mixtures were compression molded at 165°C for 5 min.

To prepare nanocomposite foams, LLDPE, clay, Organosilane, zinc oxide (3 phr), and stearic acid (1 phr) were mixed in a Haake internal mixer at 165°C

Correspondence to: G.-H. Kim (guehyun@gdsu.dongseo.ac.kr).

Contract grant sponsor: Dongseo University.

**TABLE I**  
**Important Characteristics of the Materials Used in this Study**

Class of materials	Materials	Supplier	Characteristics
Polymer Clay	LLDPE	Mitsui Chemical, Japan	ML1 + 4 (100°C) : 40
	Cloiste Na <sup>+</sup>	Southern Clay, USA	Density (g/cm <sup>3</sup> ) : 0.89
	Cloisite 20A		Modifier concentration (mequiv/100 g clay) : 95
	Cloisite 30B		Modifier concentration (mequiv/100 g clay) : 90
Crosslinking agent	Dicumyl Peroxide	Akzo Nobel, The Netherlands	
Crosslinking coagent	Zinc oxide	Gil-Chen Chem., Korea	
	Stearic acid	LG-Chem., Korea	
Blowing agent	JTR/M	Kumyang Chem., Korea	
Organosilane	Silanogran PV	Kettlitz-chemie, German	Trimethoxysilyl-modified polybutadiene (50%) on special carrier (50%)

for 5 min. Then the obtained hybrids were mixed with chemical blowing agent and crosslinking agent in a two-roll mill. JTR-M (chemical blowing agent) and DCP (crosslinking agent) content was fixed at 5 phr and 1phr, respectively, based on the total amount of LLDPE. The chemical blowing agent used was azodicarbonamide-based blowing gas release system (JTR-M). Azodicarbonamide is odorless and easily dispersed. It is activated by organic acids, bases, and metal compounds. After mixing in a two-roll mill the mixture was put in a mold and the foams were obtained by compression molding. The mixture was pressed at 14.7 MPa, in a hydraulic press at 155°C for 40 min, respectively. After removal of the pressure, expansion took place immediately. Then the obtained foams were left at room temperature for at least 24 h before any sample preparation. All of the skin is removed from the foam before testing.

### Nanocomposite testing

X-ray diffraction (XRD) studies were conducted by a Rigaku D/max 2200H X-ray diffractometer (40 kV, 50 mA, Cu-K $\alpha$  radiation). The scanning rate was 0.5°/min. The basal spacing of silicate layer,  $d$ , was calculated using the Bragg's equation,  $n\lambda = 2d\sin\theta$ . Transmission electron microscopy (TEM) images were taken from cryogenically microtomed ultra thin sections using EF-TEM (EM 912 Omega).

A Universal Testing Machine (Model 4466, Instron Co.) was used to obtain the tensile properties of the nanocomposites at room temperature. The crosshead speed was 500 mm/min. All measurements were performed for five replicates of dog-bone shaped specimens and averaged to get the final result.

Thermal stability of nanocomposites was studied through thermogravimetric analysis (TGA 2050, TA Instrument) under nitrogen atmosphere. The heating rate was 10°C/min. For DSC (DSC 2010, TA Instrument) measurements, the temperature was calibrated using standard materials. The samples with a

typical mass of 10 mg were encapsulated in sealed aluminum pans. The DSC measurements were conducted under nitrogen atmosphere. The heating and cooling rate was fixed at 10°C/min. The first cooling and second heating DSC traces were used for analysis.

Compressions set measurements were performed according to ASTM D395. The foams were compressed by 50% for 6 h at 50°C and then the pressure was removed and the foam was allowed to recover for 30 min at ambient temperature. The final sample thickness was measured and the compression set was calculated using the following equation.

$$\text{Compression set (\%)} = [(T_o - T_f)/(T_o - T_s)] \times 100$$

where  $T_o$  = Original sample thickness,  $T_f$  = Final sample thickness,  $T_s$  = Spacer thickness.

To investigate cellular structure, cross sections of the LLDPE based foams were cryogenically microtomed and were examined with FEG-Scanning Electron Microscope (SEM, Quanta 200FEG). About 250 cells in each SEM image were analyzed to obtain average cell size and cell density. The cell size was determined by measuring the maximum diameter of each cell. The cell density ( $N_f$ ), the number of cells per unit volume, is determined from eq. (1)<sup>22</sup>:

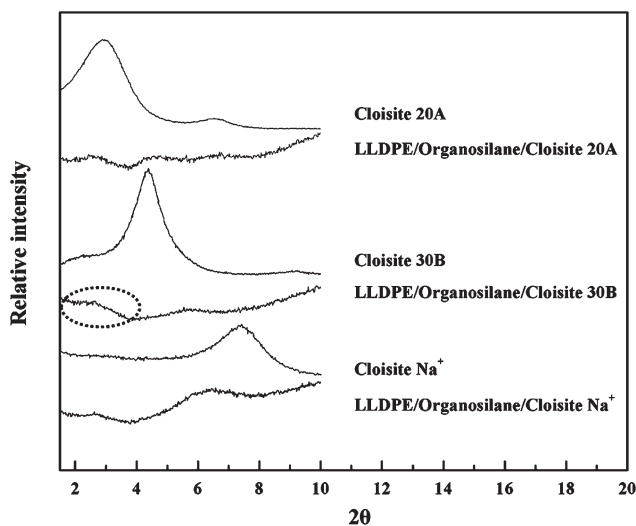
$$N_f = (nM^2/A)^{3/2} \quad (1)$$

where  $n$  is the number of cells on the SEM micrograph,  $M$  the magnification factor,  $A$  the area of the micrograph (cm<sup>2</sup>).

## RESULTS AND DISCUSSION

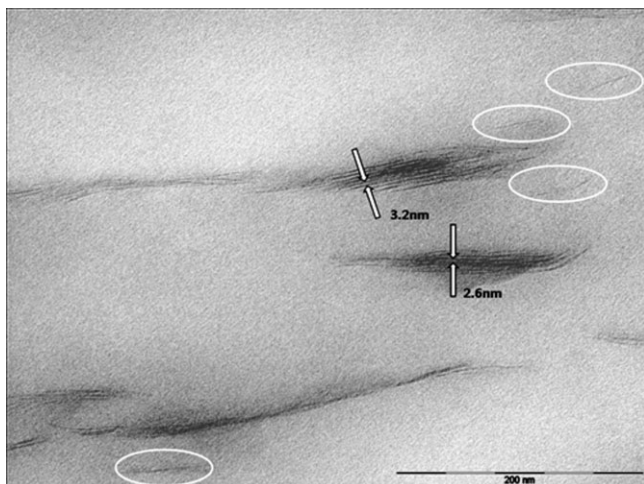
### Characterization of nanocomposites

Figure 1 shows the XRD patterns of LLDPE/Organosilane/clay nanocomposites. DCP, Organosilane, and clay content were fixed at 1.0 phr, 0.5 phr, and



**Figure 1** XRD patterns of LLDPE/Organosilane/clay (100/0.5/3 phr) nanocomposites.

3 phr, respectively. For LLDPE/Organosilane/Cloisite Na<sup>+</sup> composite, the peak position shifts at a slightly lower angle ( $d_{001}$  : 13Å) compared with original Cloisite Na<sup>+</sup> ( $d_{001}$  : 12Å). This indicates nearly no intercalation of polymers into the inter-layer of Cloisite Na<sup>+</sup>. For LLDPE/Organosilane/Cloisite 30B nanocomposite, only small bump (indicated by circle) is observed at a smaller angle compared with original Cloisite 30B ( $d_{001}$  : 19 Å). This indicates the intercalation of polymers into the inter-layer of Cloisite 30B. For LLDPE/Organosilane/Cloisite 20A nanocomposite, there is no apparent diffraction peak existing. This may indicate the coexistence of intercalated and exfoliated Cloisite 20A. Based on these results, it can be concluded that Cloisite 20A is the better choice than Cloisite Na<sup>+</sup> and Cloisite 30B and Organosilane can be used as a com-



**Figure 2** TEM photograph of LLDPE/Organosilane/Cloisite 20A (100/0.5/3 phr) nanocomposite.

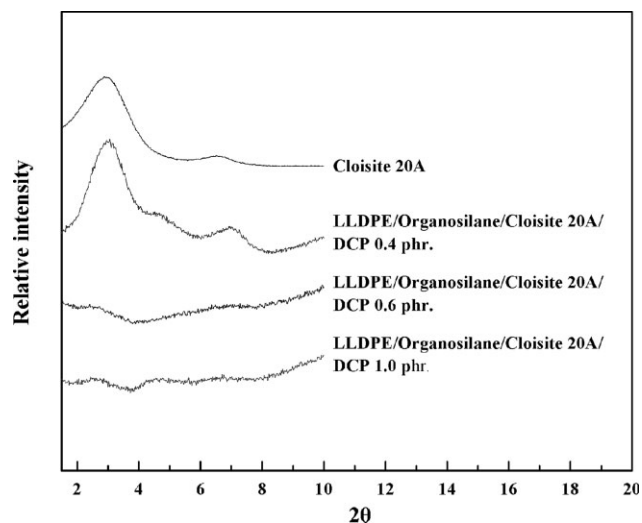


**Figure 3** XRD patterns of LLDPE/Organosilane/Cloisite 20A (100/0.5/3 phr) nanocomposites with various DCP content.

patibilizer. Because LLDPE has no polar groups, the most hydrophobic clay, Cloisite 20A seems naturally the better choice.

To visualize the dispersion of clays directly in LLDPE/Organosilane/Cloisite 20A nanocomposites, TEM studies were carried out. Figure 2 presents the typical TEM photographs of an ultra-thin section of the LLDPE/Organosilane/Cloisite 20A nanocomposite. Both intercalated and exfoliated morphologies are observed in TEM that supports the XRD findings. The exfoliated layers are indicated by circle.

Figure 3 shows the XRD patterns of LLDPE/Organosilane/Cloisite 20A nanocomposites prepared with various DCP concentrations. Organosilane and Cloisite 20A content was fixed at 0.5 phr and 3 phr. For DCP 0.4 phr, the peak position remains nearly same as original Cloisite 20A. For DCP 0.6 phr, only

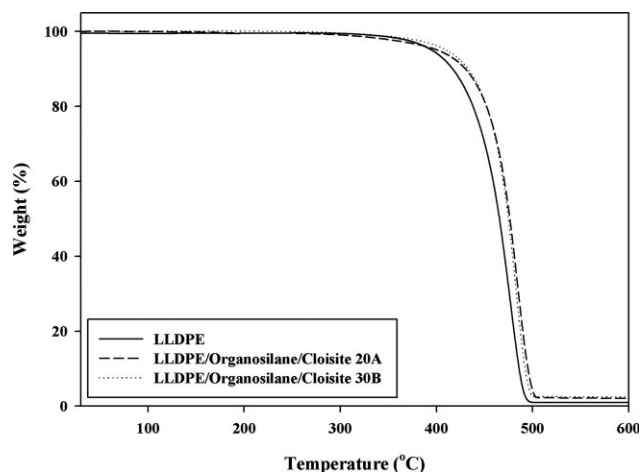


**Figure 4** TGA curves of LLDPE and LLDPE/Organosilane/clay (100/0.5/3 phr) nanocomposites.

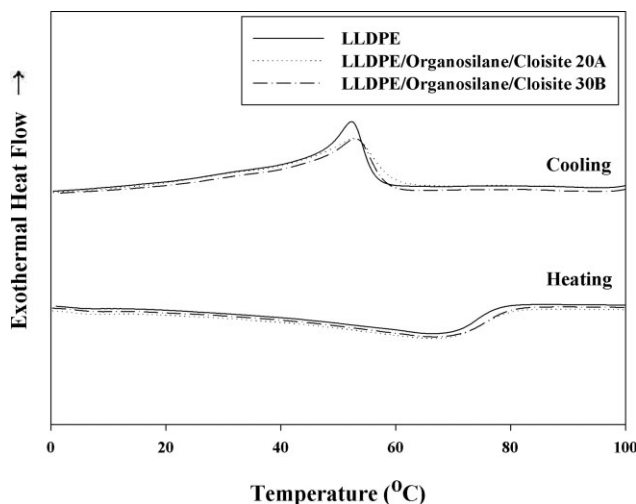


**Figure 5** DSC thermodiagrams of LLDPE and LLDPE/Organosilane/clay (100/0.5/3 phr) nanocomposites.

small bump is observed at a smaller angle compared with original Cloisite 20A. For DCP 1.0 phr, there is no apparent diffraction peak existing. With increasing DCP concentration from 0.4 phr to 1.0 phr, more polymer intercalation into the clays occurs. Generally with increasing DCP concentration, the grafting yield of Organosilane to the LLDPE increases. Because the LLDPEs grafted with more Organosilane are more hydrophilic, more polymer intercalation may occur.

Figure 4 shows the TGA curves of LLDPE and LLDPE/Organosilane/clay (100/0.5/3 phr) nanocomposites. LLDPE/Organosilane/clay nanocomposites exhibit better thermal stability than LLDPE. Figure 5 shows the DSC thermodiagrams for LLDPE and LLDPE/Organosilane/clay (100/0.5/3 phr) nanocomposites at a scan rate of 10°C/min. The crystallization temperature of LLDPE/Organosilane/

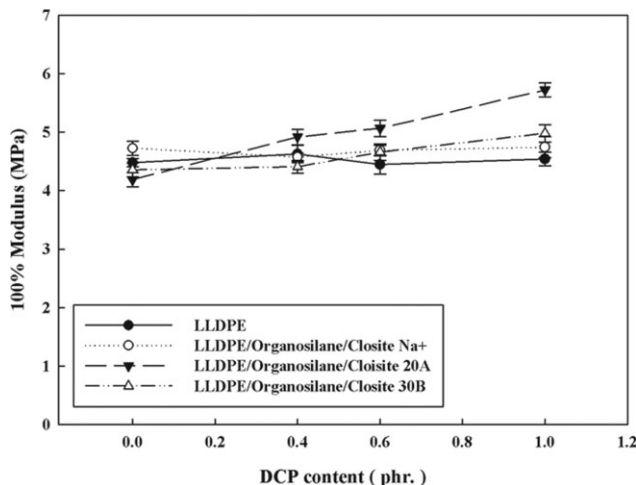


**Figure 6** One hundred percent tensile modulus of LLDPE/Organosilane/clay (100/0.5/3 phr) nanocomposites.

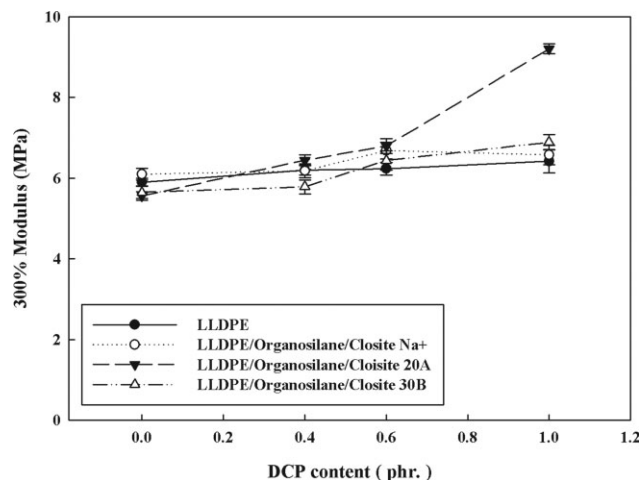


**Figure 7** Three hundred percent tensile modulus of LLDPE/Organosilane/clay (100/0.5/3 phr) nanocomposites.

clay nanocomposites is higher than that of LLDPE. Clay can provide nucleating sites in the heterogeneous nucleating process. However, the addition of clay to LLDPE has almost no effect on melting peak temperature of LLDPE. Also, adding clay to LLDPE does not lead to significant change of  $\Delta H$  of LLDPE.

### Mechanical properties

Figures 6-8 show 100%, 300%, and 500% tensile modulus for LLDPE/Organosilane/clay nanocomposites, respectively. The content of Organosilane was fixed at 0.5 phr. Generally in composites, their modulus is related to the dispersion of fillers and interaction between fillers and matrix. Well-dispersed fillers and high interaction between fillers and matrix give higher enhancement of modulus to the composites.<sup>23-25</sup> Based on modulus results, Cloisite

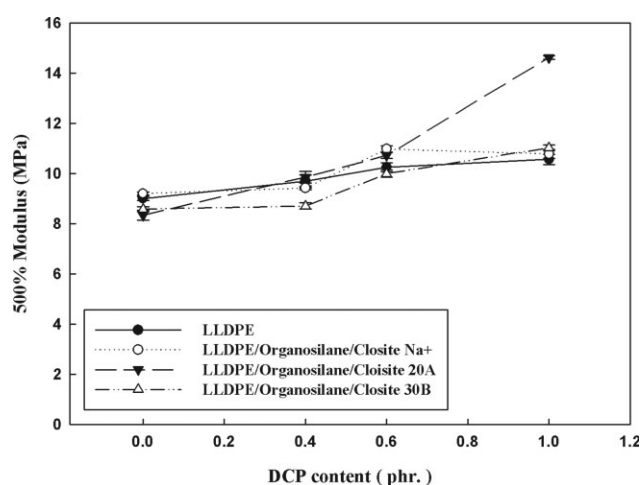


**Figure 8** Five hundred percent tensile modulus of LLDPE/Organosilane/clay (100/0.5/3 phr) nanocomposites.

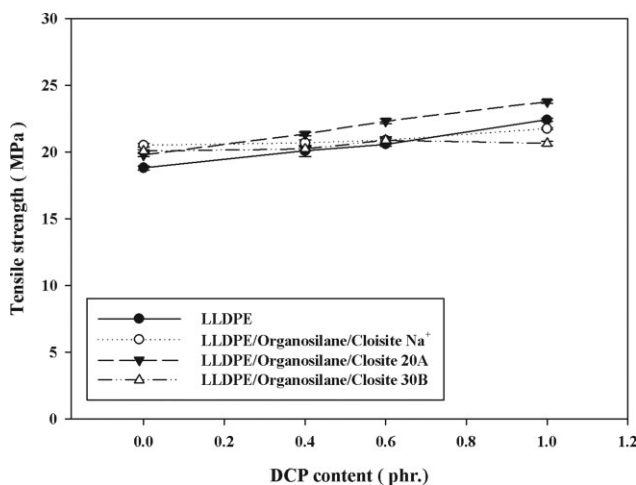


**Figure 9** Tensile strength of LLDPE/Organosilane/clay (100/0.5/3 phr) nanocomposites.

20A is the most appropriate clay for LLDPE/clay nanocomposites. This is the same conclusion with XRD results. For Cloisite 20A, the enhancement of modulus is very obvious with increasing the content of DCP. This is due to the more polymer intercalation into the interlayer of Cloisite 20A and higher cross-linking density. More polymer intercalation with increasing DCP concentration was also confirmed with XRD results (Fig. 3). With increasing DCP concentration, the grafting yield of Organosilane to the polymer LLDPE increases and more polymer intercalation may occur. Tensile strength also increases with increasing DCP concentration especially for Cloisite 20A (Fig. 9). However, elongation at break decreases with increasing DCP concentration (Fig. 10).

### Nanocomposite foams

To investigate the effect of Organosilane on the mechanical properties of nanocomposite foams,

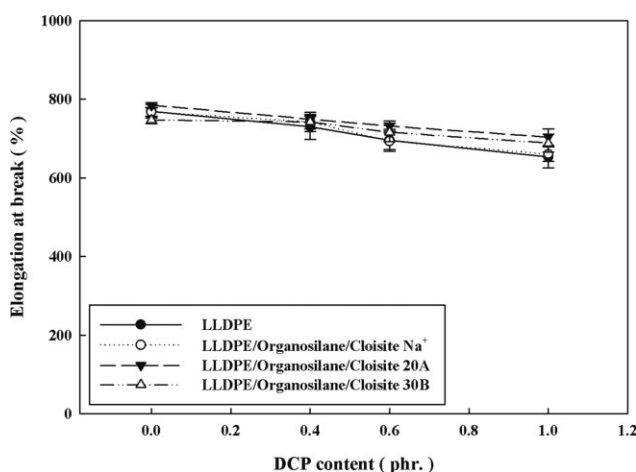


**Figure 10** Elongation at break of LLDPE/Organosilane/clay (100/0.5/3 phr) nanocomposites.

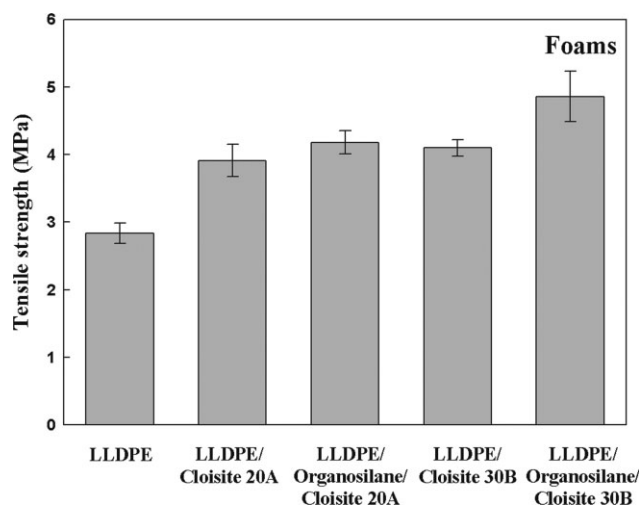


**Figure 11** Tensile strength of LLDPE and LLDPE/clay nanocomposite foams.

LLDPE/Organosilane/clay nanocomposite foams were prepared. Figure 11 shows the tensile strength of LLDPE and LLDPE/clay nanocomposite foams with same density. Tensile strength of LLDPE/clay nanocomposite foams is higher than that of LLDPE foams. With addition of Organosilane to LLDPE/clay foams, the tensile strength of nanocomposite foams further increases. 100% tensile modulus also displays similar trends and LLDPE/Organosilane/Cloisite 20A displays the highest 100% tensile modulus (Fig. 12). Elongation at break of LLDPE/Organosilane/Cloisite 20A foams is lower than that of LLDPE/Cloisite 20A foams (Fig. 13). However, elongation at break of LLDPE/Organosilane/Cloisite 30B foams is higher than that of LLDPE foams. Compression set of LLDPE/Cloisite 20A foam and LLDPE/Cloisite 30B foam is higher than that of LLDPE foam (Fig. 14). Compression set is the reduction in

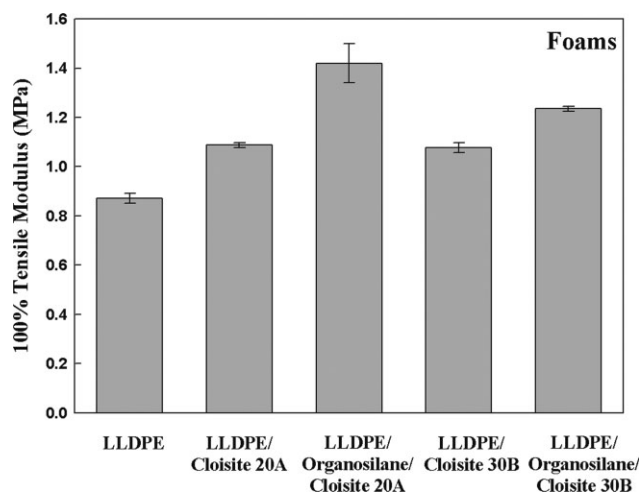


**Figure 12** One hundred percent tensile modulus of LLDPE and LLDPE/clay nanocomposite foams.

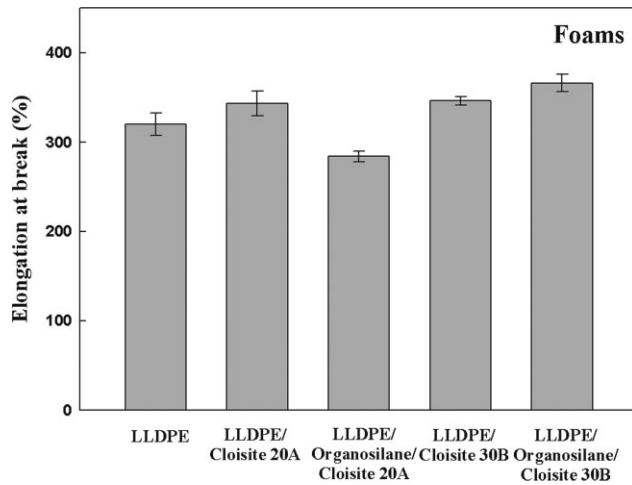
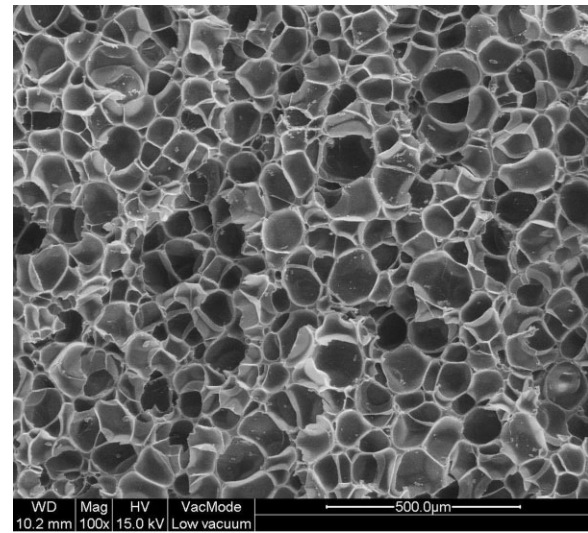


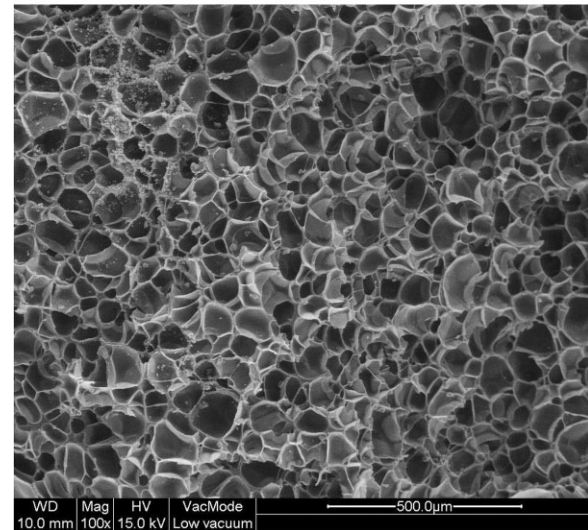
**Figure 13** Elongation at break of LLDPE and LLDPE/clay nanocomposite foams.

thickness after a material is aged in compression. The viscoelastic recovery of the bent cell walls is the main mechanism that controls the recovery of the samples. The plastic buckling of cell walls and energy dissipation by the chain slipping may lead to reduction in thickness after aging in compression. The lower the compression set the better the elastic recovery of the foam. LLDPE/Organosilane/clay nanocomposite foams exhibit better compression set property than LLDPE/clay nanocomposite foams.

Figure 15 shows typical SEM images of the cellular structure of the LLDPE and LLDPE/Cloisite 20A foams. The foams have a closed-cell structure. Figure 16 shows the cell size and cell density for the foams. Compared with LLDPE foams, there is a big



(a)



(b)

**Figure 15** Typical SEM images of the cellular structure: (a) LLDPE foam, (b) LLDPE/Cloisite 20A foam.

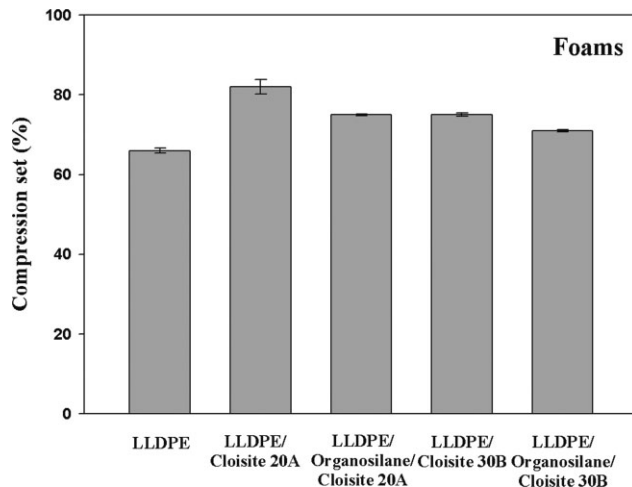


**Figure 14** Compression set of LLDPE and LLDPE/clay nanocomposite foams.

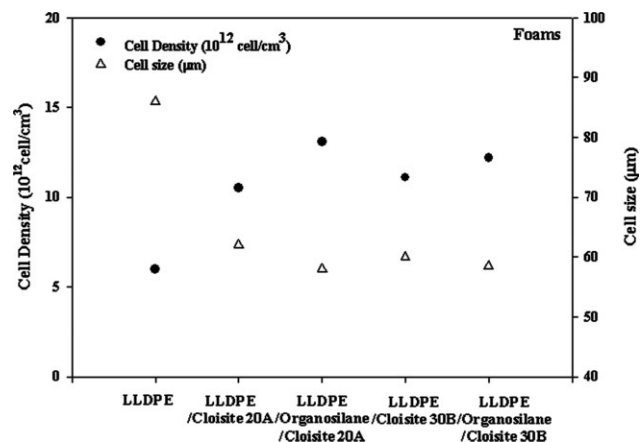


**Figure 16** Cell size and cell density for LLDPE and LLDPE/clay nanocomposite foams.

decrease in cell size but a big increase in cell density in LLDPE/Cloisite 20A and LLDPE/Cloisite 30B foams. The decrease in cell size is because of the higher melt viscosity of the materials during foam processing. The melt viscosity increases with addition of clay.<sup>26</sup> Generally, the residues of chemical blowing agent act as nucleating agents. Similarly, clay can provide nucleating sites in the heterogeneous nucleating process, leading to the increase in cell density in this study. The addition of Organosilane to LLDPE/clay foams leads to the further decrease in cell size and increase in cell density.

### CONCLUSIONS

There is no apparent diffraction peak existing in the XRD patterns of LLDPE/Organosilane/Cloisite 20A nanocomposite (DCP : 1.0 phr and Organosilane: 0.5 phr). This indicates the coexistence of intercalated and exfoliated Cloisite 20A. Since it is very difficult for hydrophobic polymers such as LLDPE to intercalate into clays, a compatibilizer should be used in hydrophobic polymer/clay nanocomposites. Currently, maleic anhydride grafted polyethylenes have been dominantly used for polyethylene/clay nanocomposites as compatibilizers. Based on this study, it can be concluded that Organosilane is also a very good compatibilizer. However, it is found that appropriate amount of DCP should be used with Organosilane and in this study DCP should be used at least above 0.6 phr for 0.5 phr of Organosilane. Organosilane was also confirmed as a good compatibilizer in preparing LLDPE/clay nanocomposite foams.

### References

1. Alexandre, M.; Dubois, P. *Mater Sci Eng* 2000, 28, 1.
2. Lebaron, P. C.; Wang, Z.; Pinnavaia, T. J. *Appl Clay Sci* 1999, 15, 11.
3. Giannelis, E. P. *Adv Mater* 1996, 8, 29.
4. Ray, S. S.; Okamoto, M. *Prog Polym Sci* 2003, 28, 1539.
5. Arroyo, M.; López-Manchado, M. A.; Herrero, B. *Polymer* 2003, 44, 2447.
6. Zhang, L.; Wang, Y.; Wang, Y.; Sui, Y.; Yu, D. *J Appl Polym Sci* 2000, 78, 1873.
7. Ganter, M.; Gronski, W.; Reichert, P.; Mülhaupt, R. *Rubber Chem Technol* 2001, 74, 221.
8. Kim, J. T.; Oh, T. S.; Lee, D. H. *Polym Int* 2003, 52, 1058.
9. Kim, J. T.; Lee, D. Y.; Oh, T. S.; Lee, D. H. *J Appl Polym Sci* 2003, 89, 2633.
10. Vu, Y. T.; Mark, J. E.; Pham, L. H.; Engelhardt, M. *J Appl Polym Sci* 2001, 82, 1391.
11. Varghese, S.; Karger-Kocsis, J.; Gatos, K. G. *Polymer* 2003, 44, 3977.
12. Usuki, A.; Tugigase, A.; Kato, M. *Polymer* 2002, 43, 2185.
13. Shieh, Y. T.; Tsai, T. H. *J Appl Polym Sci* 1998, 69, 255.
14. Shieh, Y. T.; Liu, C. M. *J Appl Polym Sci* 1999, 74, 3404.
15. Parent, J. S.; Geramita, K.; Ranganathan, S.; Whitney, R. A. *J Appl Polym Sci* 2000, 76, 1308.
16. Sirisinha, K.; Meksawat, D. *J Appl Polym Sci* 2004, 93, 901.
17. Sirisinha, K.; Meksawat, D. *J Appl Polym Sci* 2004, 93, 1179.
18. Kuan, H. C.; Kuan, J. F.; Ma, C. C. M.; Huang, J. M. *J Appl Polym Sci* 2005, 96, 2383.
19. Sirisinha, K.; Meksawat, D. *Polym Int* 2005, 54, 1014.
20. Lu, H.; Hu, Y.; Li, M.; Chen, Z.; Fan, W. *Compos Sci Technol* 2006, 66, 3035.
21. Lu, H.; Yuan, H.; Ling, Y.; Zhengzhou, W.; Zuyao, C.; Weicheng, F. *J Mater Sci* 2005, 40, 43.
22. Han, X.; Zeng, C.; Lee, L. J.; Koelling, K. W.; Tomasko, D. L. *Polym Eng Sci* 2003, 43, 1261.
23. Malucelli, G.; Ronchetti, S.; Lak, N.; Priola, A.; Dintcjeva, N. T.; Mantia, F. P. L. *Eur Polym J* 2007, 43, 328.
24. Liang, G.; Xu, J.; Bas, S.; Xu, W. *J Appl Polym Sci* 2004, 91, 3974.
25. Morawiec, J.; Pawlak, A.; Slouf, M.; Galeski, A.; Piorkoska, E.; Krasnikowa, N. *Eur Polym J* 2005, 41, 1115.
26. Gopakumar, T. G.; Lee, J. A.; Kontopoulou, M.; Parent, J. S. *Polymer* 2002, 43, 5483.